8-10-2020

Metabolomics Analysis of Annual Killifish (austrofundulus Limnaeus) Embryos During Aerial Dehydration Stress

Daniel Zajic
Portland State University

Jason Podrabsky
Portland State University, podrabsj@pdx.edu

Citation Details

Published as: Zajic, D. E., & Podrabsky, J. E. (2020). Metabolomics analysis of annual killifish (Austrofundulus limnaeus) embryos during aerial dehydration stress. *Physiological Genomics*. https://doi.org/10.1152/physiolgenomics.00072.2020

Metabolomics analysis of annual killifish (*Austrofundulus limnaeus*) embryos during aerial dehydration stress

Daniel E. Zajic[1,2]* and Jason E. Podrabsky[1]

[1]Department of Biology, Portland State University, P.O. Box 751, Portland, OR 97207
[2]Health, Human Performance, and Athletics Department, Linfield University, 900 SE Baker, McMinnville, OR 97128

***Corresponding author:**
dzajic@linfield.edu
Health, Human Performance, and Athletics Department
Linfield University
900 SE Baker
McMinnville, OR 97128

Key words: diapause, antioxidants, 2-hydroxyglutarate, lanthionine, neuroprotection

Running title: Metabolomics of dehydrated killifish embryos

Author contributions

Conceptualization: D.E.Z., J.E.P.; Methodology: D.E.Z., J.E.P.; Formal analysis: D.E.Z., J.E.P.; Investigation: D.E.Z., J.E.P.; Data curation: D.E.Z., J.E.P.; Writing - original draft: D.E.Z.; Writing - review & editing: D.E.Z., J.E.P.; Visualization: D.E.Z., J.E.P.; Supervision: J.E.P.; Funding acquisition: J.E.P.

Abstract

The annual killifish, *Austrofundulus limnaeus*, survives in ephemeral ponds in the coastal deserts of Venezuela. Persistence through the dry season is dependent on drought-resistant eggs embedded in the pond sediments during the rainy season. The ability of these embryos to enter drastic metabolic dormancy (diapause) during normal development enables *A. limnaeus* to survive conditions lethal to most other aquatic vertebrates; critical to the survival of the species is the ability of embryos to survive months and perhaps years without access to liquid water. Little is known about the molecular mechanisms that aid in survival of the dry season. This study aims to gain insight into the mechanisms facilitating survival of dehydration stress due to aerial exposure by examining metabolite profiles of dormant and developing embryos. There is strong evidence for unique metabolic profiles based on developmental stage and length of aerial exposure. Actively developing embryos exhibit more robust changes, however, dormant embryos respond in an active manner and significantly alter their metabolic profile. A number of metabolites accumulate in aerial-exposed embryos that may play an important role in survival, including the identification of known antioxidants and neuroprotectants. In addition, a number of unique metabolites not yet discussed in the dehydration literature are identified, such as lanthionine and 2-hydroxyglutarate. Despite high oxygen availability, embryos accumulate the anaerobic end-product lactate. This paper offers an overview of the metabolic changes occurring that may support embryonic survival during dehydration stress due to aerial incubation, which can be functionally tested using genetic and pharmacological approaches.

Introduction

The annual killifish, *Austrofundulus limnaeus*, inhabits temporary pools in the Maracaibo basin of Venezuela. Their habitat is defined by highly unpredictable episodic rain events, which leads to uncertainty in the length of time that a pool will experience inundation. Thus, individual pools may remain dry for months or perhaps years (44, 50, 52). During the rainy season, adult *A. limnaeus* deposit their embryos into the often oxygen-limited pool substrate. As the rainy season ends, the adult fish die and embryos must survive severely dehydrating conditions in the mud, often faced with a variety of other stresses such as extremes in temperature and oxygen until the wet season returns and they can complete development (44). As a result, *A. limnaeus* has evolved extremely stress-resistant embryos with the ability to enter a profound state of metabolic depression termed diapause (48, 49). There are three unique stages of diapause (I, II, and III) which an embryo can enter during development (43, 70, 71). The most stress-tolerant stage, diapause II (DII), occurs midway through development and mostly consists of cardiac and neural tissue (48, 51). The developmental ecology of *A. limnaeus* embryos has not been characterized in the field. However, embryos of other species of annual killifish are primarily found in DII during the peak of the dry season, and in a variety of post-DII stages during the late dry season (53). Thus, DII is likely primarily responsible for dry season survival in *A. limnaeus,* but tolerance of dehydrating conditions is required during the entire duration of post-DII development.

For aquatic organisms, aerial exposure imposes oxygen stress due to an increase in availability compared to most aquatic habitats, but also imposes a severe dehydration stress. A main reason for dehydration injury is attributed to the increased formation of ROS and subsequent oxidative damage due to water stress (14). Free radical formation can lead to lipid peroxidation, denaturation of proteins, and DNA damage which ultimately can affect overall metabolism (18). However, protection against such damage can partially be mitigated by accumulation of antioxidant metabolites, such as glutathione (GSH) (30). Embryos of *A. limnaeus* have a notable tolerance of oxidative stress (65), but the role of antioxidants has not been investigated through the lens of dehydration stress.

Embryos of *A. limnaeus* experience unique resistance to dehydration stress that is not seen in other aquatic vertebrates and can survive for over 500 days at 85% relative humidity (RH) (46, 74); however, this ability has received far less attention than other aspects of their biology. When embryos of *A. limnaeus* are aerially incubated, thus exposed to dehydration stress, they initially lose water from the extraembryonic perivitelline space but embryonic compartments remain fully hydrated (46). After a week, water loss approaches zero. Paradoxically, DII embryos respond to aerial dehydration stress by increasing oxygen consumption, while post-diapause II (post-DII) embryos are either unaffected or severely reduce oxygen consumption. The mechanisms that aid survival during dehydration stress and contribute to these metabolic phenotypes are unknown.

Austrofundulus limnaeus is a promising model organism for developmental physiology and ecology because of their tolerance of a plethora of stresses, annotated genome, and ability to alter developmental trajectories in the lab (43, 47, 54, 64). The current study was performed to expand our knowledge of stress tolerance in *A. limnaeus* by exploring the metabolic pathways that may be providing this species with its remarkable abilities to survive extreme dehydration stress. We examine the metabolite profiles of dormant (DII) and actively developing (post-DII) embryos in response to short and long-term aerial dehydration stress (85% RH). We show that actively developing and dormant embryos share metabolic pathways and accumulation of similar metabolites in response to dehydration stress. However, we also see developmentally distinct differences that suggest stage-specific responses. We identify critical roles for amino acid and lipid metabolism, show accumulation of known antioxidant and neuroprotective compounds, and identify novel metabolites produced in response to aerial dehydration stress.

Materials and Methods

Animal husbandry and embryo collection

Adult annual killifish were housed and embryos collected as previously described (45). All work was performed under established protocols that were reviewed and sanctioned by the Portland State University Institutional Animal Care and Use Committee (PSU IACUC protocols #33 and 64). Briefly, adult fish were kept in male-female pairs and spawned semiweekly. Embryos were collected and stored at 25°C with no light in 15 x 100 mm plastic Petri dishes in media that resembles the environmental conditions from which adults were collected in 1995 (10 mmol l^{-1} NaCl, 2.15 mmol l^{-1} $MgCl_2$, 0.8 mmol l^{-1} $CaCl_2$, 0.14 mmol l^{-1} KCl, 1.3 mmol l^{-1} $MgSO_4$) (45, 50). For the first 4 days post-fertilization (dpf), embryo medium contained methylene blue (0.0001%) to prevent fungal infection. Embryos were then treated with two 5 min washes of a 0.01% sodium hypochlorite solution (separated by a 5 min rest in embryo medium) to prevent bacterial and fungal growth, as previously described (45). Following sodium hypochlorite treatment, embryos were transferred to embryo medium containing 10 mg l^{-1} gentamicin sulfate and allowed to develop to DII (32–64 d). To break DII, embryos were subjected to a temperature of 30°C and full spectrum light for 48 h (31). Following this treatment, embryos were sorted into synchronized cohorts of embryos by developmental stage (Wourms' stage [WS]) as described in Podrabsky et al. (43).

Embryonic stages investigated

Experiments were performed on dormant (DII) and actively developing post-DII embryos (43, 70, 71) to identify stage-specific responses to dehydration stress and to capture different levels of dehydration tolerance. DII embryos are metabolically dormant, have halted development, and have a lethal time to 50% mortality (LT_{50}) in aerial incubation (85% relative humidity [RH]) of 325 d (74). DII embryos tend to stay in diapause during aerial exposure. Post-DII embryos are metabolically active, continue developing during aerial exposure when oxygen is not limiting, and have reduced tolerance of dehydrating conditions. When exposed to aerial conditions during early post-DII development (WS 36, 4 days post-diapause II), dehydration tolerance is reduced to an LT_{50} of 84 d. Late

post-DII embryos (WS 40–42) have a further reduced ability to survive aerial incubation and exhibit LT_{50} values around 28–29 d (74).

Metabolomics analysis

Aerial incubation

Embryos were exposed to 85% relative humidity (RH) air at 25°C with no light in a sealed glass desiccator with a porcelain plate shelf (250 mm diameter, 08615B, Fisher Scientific, Hampton, NH, USA). Relative humidity was controlled by using a saturated solution of potassium chloride (750 ml) placed below the shelf and continually mixed with a stir bar to ensure uniform RH within the aerial portion of the chamber (46, 68). Prior to exposure, embryos were treated with sodium hypochlorite (see above) and incubated in embryo medium containing 10 mg l^{-1} gentamicin sulfate for 3 h prior to aerial exposure. Embryos were placed on filter pads containing 2.5 ml embryo medium containing gentamicin. Care was taken to make certain that single embryos were isolated and not touching other embryos. Embryos were then exposed to 85% RH at 25°C without light. DII embryos were sampled after 7 and 28 d while post-DII embryos were sampled at 7 (WS 40) and 18 d (WS 42/43). Control embryos (DII and WS 36) were collected at t = 0 by quickly blotting away embryo medium prior to sampling. Six biological replicates (*N* = 6), comprised of 25 embryos each, were flash frozen with liquid N_2 and stored at –80°C until shipped to Metabolon for metabolite profiling. To better visualize the sampling regimen, see **Figure 1.**

Metabolon metabolomics analysis

Sample preparation and metabolomics analysis occurred at Metabolon, but is briefly detailed here. Samples were prepared using an automated MicroLab STAR system (Hamilton Company, Reno, NV, USA). Proteins were precipitated with methanol under vigorous shaking for 2 min (Glen Mills GenoGrinder 2000) followed by centrifugation. This method ensured dissociation of small molecules bound to protein, trapped in the precipitated protein matrix, and recovery of chemically diverse metabolites. The resulting extract was divided into four fractions: two for analysis by two separate reverse phase (RP)/UPLC-MS/MS methods with positive ion mode electrospray ionization (ESI),

one for analysis by RP/UPLC-MS/MS with negative ion mode ESI, and one for analysis by HILIC/UPLC-MS/MS with negative ion mode ESI. To remove methanol, samples were placed briefly on a TurboVap (Zymark, Hopkinton, MA, USA). The sample extracts were stored overnight under nitrogen before preparation for analysis. Prior to analysis, sample extracts were reconstituted in solvents compatible to each of the four methods described above. Raw data was extracted, peak-identified, and quality control processed using Metabolon's proprietary hardware and software. At the time of analysis, identification of known biochemicals was based on comparison to metabolomic libraries of more than 3300 commercially available purified standard compounds. Several curation procedures were carried out to ensure high quality data and removal of those data representing system artifacts, mis-assignments, and background noise. The present dataset comprises a total of 673 compounds of known identity (metabolites). Data for each metabolite is presented relative to control samples (t = 0) and expressed as non-normalized, protein-normalized (Bradford assay), and DNA-normalized (Table 1). Due to the changing amount of water in the samples over the course of aerial incubation, and continued development in post-DII embryos, we have chosen to use the DNA-normalized data to most accurately reflect the relative amounts of metabolites per cell. Bradford protein concentration increases in a linear manner during dehydration while at the same time embryo mass decreases in a similar manner (Supplemental Fig S1; for all supplementary material see https://doi.org/10.6084/m9.figshare.12502085). We interpret this pattern as an artifact of water loss (especially in the DII embryos which are dormant) and so normalization per protein would exaggerate fold changes.

Statistical analysis

Graphical and statistical analyses were performed using Prism 8.0 software (GraphPad, La Jolla, CA, USA) or through Metabolon's user interface. Statistical significance was set to $P < 0.05$ for all comparisons. For metabolomics data analysis, missing values due to being under the limit of detection of the instruments were imputed with the minimum value on a per metabolite basis. For each metabolite, raw counts were scaled to set the median across all samples for that metabolite to 1 and the data log transformed.

Following normalization to Bradford protein or DNA concentration, Welch's two-sample *t*-test was used to identify metabolites that differed significantly between treatments, with a threshold for statistical significance set to $P < 0.05$. Additionally, an estimate of the false discovery rate (*q*-value) was calculated to take into account the multiple comparisons that normally occur in metabolomic-based studies. A low *q*-value ($q < 0.10$) is an indication of high confidence in a result. Thus, only metabolites with $P < 0.05$ and $q < 0.10$ are considered significant in this study. Pathway enrichment analysis was performed using MetaboLync (Metabolon Inc.) with all metabolites and their pre-assigned pathways as background and reference pathways, respectively. Enriched pathways were calculated based on the following formula, where significance was defined as $P < 0.05$:

$$\text{Enrichment value} = (k/m)/((n-k)/(N-m))$$

Where: k, total number of significant metabolites in pathway; m, total number of detected metabolites in pathway; n, total number of significant metabolites; N, total number of detected metabolites in the study. A pathway enrichment value greater than one indicates that the pathway contains more significantly changed compounds relative to the study overall. Fisher's exact test ($P < 0.05$) was used to determine if pathway enrichment was significant.

Results and Discussion

This is the first metabolomics study to explore the profound ability of *A. limnaeus* embryos to survive prolonged aerial dehydration stress. The metabolic profiles of DII and post-DII embryos vary greatly, but due to continued development of post-DII embryos during dehydration stress, we cannot confirm if the metabolites accumulated in post-DII embryos are dehydration-specific or developmentally regulated. It is also important to note that the levels of metabolites reported in this paper are from whole embryos. The location of the metabolites, whether they be in the developing embryo, yolk, or perivitelline fluid, is not known. Recognizing the limitations of this study, we introduce new insights into survival of embryos of *A. limnaeus* to aerial dehydration stress by focusing on pathways and metabolites that change in a similar manner in both dormant (DII) and actively developing (post-DII) embryos. Below we outline metabolic pathways and metabolites of interest that may be supporting survival of *A. limnaeus* during dehydration stress induced by aerial exposure.

Metabolomics profiles overview

We measured a total of 673 metabolites of known identity (Supplemental Table S1). A summary of metabolites that achieved statistical significance ($P < 0.05$) using various methods of normalization are presented in Table 1. We provide lists of the top significantly downregulated and upregulated metabolites in response to short-term or long-term aerial incubation in DII and post-DII embryos (Supplemental Tables S2–S9). Although the method of normalization is important, it does not affect the statistical significance of the vast majority of compounds that experience large fold-changes during aerial dehydration stress (see boldface metabolites in Supplemental Tables S2–S9). Here we focus on data normalized to total DNA content to take into account the developmental changes that occur in post-DII embryos. Overall metabolite abundance was found to generally increase following aerial exposures, with the exception of short-term incubation of post-DII embryos (Table 1). These changes in metabolites, especially in DII embryos, indicate a large-scale active response to aerial dehydration stress. The

increase in some metabolites is consistent with the observed rise in oxygen consumption seen in DII embryos when exposed to aerial conditions (74).

Superpathways

Metabolites were categorized as belonging to 1 of 8 superpathways (Fig 2). Of the metabolites measured, 70% belonged to lipid (*N* = 306) and amino acid (*N* = 164) metabolism. The remaining 30% belonged to nucleotide (*N* = 70), carbohydrate (*N* = 42), cofactors and vitamins (*N* = 30), xenobiotics (*N* = 30), peptide (*N* = 20), and energy metabolism (*N* = 11). Within each superpathway, metabolites were clustered based on 81 subpathways (Fig 2).

Enriched subpathways

Diapause II.

Seven subpathways were enriched in DII embryos following short-term aerial dehydration stress and 4 were enriched during long-term exposures (Table 2). The most enriched pathways were associated with fatty acid and amino acid metabolism. Additionally, nicotinate and nicotinamide metabolism was enriched. The amino acid subpathways enriched are shared between long-term and short-term exposures.

Post-DII embryos.

In general, there was more variation in pathway enrichment in post-DII embryos compared to DII embryos (Table 2). There were 10 enriched subpathways in response to short-term (*N* = 5) and long-term (*N* = 5) aerial incubation. Most enriched pathways belonged to lipid and amino acid metabolism. There were three pathways that were consistently enriched during short and long-term exposures: phosphatidylcholine (PC), gamma-glutamyl amino acid, and monoacylglycerol metabolism.

Shared metabolites (long-term dehydration)

Due to continued development of post-DII embryos during dehydration exposure, we chose to focus on metabolites that showed shared responses (upregulation or downregulation) in DII and post-DII embryos in response to aerial dehydration stress.

Since DII embryos remained in diapause, we can more easily attribute metabolic change as primarily a direct response to dehydration stress and not an effect of active development. DII embryos have a suppressed metabolism, thus changes in metabolic profiles may not be apparent after short-term incubation. We therefore chose to focus on metabolites shared following long-term exposures.

When compared to controls, there were a total of 71 shared metabolites that significantly increased during long-term exposures (Fig 3); whereas there were only 18 metabolites that decreased (Fig 3). Of the metabolites that increased, 48 belonged to lipid (*N* = 24) and amino acid (*N* = 24) metabolism. The remainder belonged to carbohydrate (*N* = 8), nucleotide (*N* = 7), xenobiotics (*N* = 6), cofactors and vitamins (*N* = 1), and peptide metabolism (*N* = 1). Of the metabolites that decreased, a majority belonged to monoacylglycerol metabolism (*N* = 11). The remaining downregulated metabolites belonged to nucleotide (*N* = 2), cofactors and vitamins (*N* = 2), amino acid (*N* = 1), carbohydrate (*N* = 1), and xenobiotics (*N* = 1) metabolism.

Many of these metabolites are in pathways found to be enriched in response to short or long-term aerial incubation (Table 2). In addition to those enriched pathways, there are several metabolites that belong to shared pathways that will be explored further below.

Pathways of interest

Amino acids and dipeptides

Methionine, Cysteine, and Gamma-Glutamyl Amino Acids. There are indications of altered transsulfuration activity and antioxidant demand and utilization in embryos exposed to aerial dehydration stress (Fig 4). Transsulfuration is a highly conserved pathway involved in metabolizing sulfur-containing amino acids such as methionine and cysteine. Methionine, via the transsulfuration pathway, can be converted to cysteine and several other compounds that play roles in redox balance and antioxidant defense (e.g., glutathione, taurine, etc.). Notably, an increase in cystathionine is observed in both DII and post-DII embryos (Figs 3,4).

The metabolite with the largest fold-change in this study is lanthionine (Fig 3; greater than 800-fold increase in post-DII embryos). Lanthionine is formed when

cysteine is metabolized in lieu of homocysteine or cystathionine by the transsulfuration pathway enzymes cystathionine β-synthase (CBS) and cystathionine γ-lyase (CSE) (Fig 4). A common product of lanthionine biosynthesis is hydrogen sulfide (H_2S), which has been recognized as an important biological signaling molecule (11, 38). H_2S has been shown to protect heart mitochondrial function during ischemic events and induce a state of suspended animation associated with a lower metabolism and body temperature in mice (4, 11). In addition, lanthionine can also be further metabolized in mammalian brain tissue to form the cyclic thioether, lanthionine ketimine, which is known to be associated with high affinity (58 nmol) to neuronal membranes (13) and has been demonstrated to have neuroprotective, neurotrophic and anti-inflammatory activities in mice during cerebral ischemia (19, 35). Embryos of *A. limnaeus* may experience dehydrating conditions for months and perhaps years before water returns (44, 52) and very likely depend on suppression of metabolism and induction of cellular protective mechanisms for survival (74). Thus, it is possible that lanthionine accumulation may support long-term survival of dehydration stress through suppression of metabolism mediated by H_2S production, and through the cytoprotective actions of lanthionine ketimine in cardiac and neural tissues.

The large observed increase in lanthionine suggests a potential role as a compatible osmolyte. However, in the relatively few studies that exist, elevated lanthionine (0.3–2 μmol l^{-1}) appears to have generally negative effects on fish embryo physiology and development, though some of these effects were counteracted with addition of glutathione (42). Lanthionine may also interfere with angiogenic signaling, increasing intracellular calcium, and impairing H_2S production (42, 63). Thus, the ability of *A. limnaeus* embryos to tolerate such large increases in lanthionine without apparent negative effects is interesting. Although we do not know the concentrations of lanthionine in embryos of *A. limnaeus*, an 800-fold change from even the picomolar level would reach biologically relevant concentrations (42). The biology of lanthionine, and its association with survival of long-term dehydration stress warrants further investigation.

Both the oxidized and reduced forms of glutathione (GSSG and GSH, respectively) were found to be accumulated in post-DII embryos, whereas only GSSG

was increased in abundance in DII embryos. Cells use glutathione to scavenge reactive oxygen species (ROS) in order to reduce oxidative damage. A previous study showed a significant increase in total glutathione content in *A. limnaeus* embryos during post-DII development (65). However, close to 100% of the glutathione measured was in its reduced form, thus the increases in GSSG observed in this study appear to be the result of aerial incubation. In their natural habitat, *A. limnaeus* embryos are exposed to a variety of conditions (e.g. hypoxia, high temperatures) as they endure the dehydrating conditions of the dry season, which could lead to increases in ROS production. A rise in GSSG is usually indicative of some form of oxidative stress. One explanation for the observed rise in GSSG in DII embryos may be due to increased oxidative stress as a consequence of increased oxygen availability and increased oxygen consumption observed in response to aerial dehydration stress (74). Another possibility is that GSSG is assisting in reducing protein synthesis during dehydration, as GSSG is a known potent inhibitor of protein synthesis (12).

Post-DII embryos also display significant decreases in 5-oxoproline, an intermediate of gamma-glutamyl amino acid metabolism, which could be reflective of changes in glutathione recycling. Fourteen gamma-glutamyl metabolites decreased in aerially incubated post-DII embryos and not surprisingly this pathway is enriched in post-DII embryos (Table 2; Fig 5). The function of the gamma-glutamyl pathway is somewhat controversial. The original theory suggested the main function was amino acid transport into the cell via their conversion to gamma-glutamyl amino acids, a glutathione-dependent process (39). The release of amino acids from gamma-glutamyl amino acids by gamma-glutamyl cyclotransferase generates 5-oxoproline as an intermediate (Fig 4). However, recent findings suggest a role for the gamma-glutamyl cycle as a regulator of redox metabolism of free radicals and xenobiotics (22). A recent review by Bachhawat and Yadav proposes a “glutathione cycle” to replace the established gamma-glutamyl cycle (2). The discrepancies in these cycles is beyond the scope of this article, but there is a clear role for both glutathione and gamma-glutamyl metabolism in *A. limnaeus* embryos worth further exploration.

Tryptophan Metabolism. There were 2 metabolites that increased in the pathway for metabolism of tryptophan: C-glycosyltryptophan and picolinate. Of note is picolinate, which exhibited a 65-fold change in DII embryos (Fig 3; Supplemental Tables S2–5). The large increase observed in metabolically suppressed embryos suggests an important role for picolinate, a small molecule with known neuroprotective, immunological, and anti-proliferative effects (5, 17) in survival of aerial dehydration stress.

Creatine Metabolism. DII and post-DII embryos exhibited different creatine metabolite profiles (Fig 6). Creatine phosphate (PCr) serves as a diffusible high-energy phosphate reserve in vertebrate cells. The accumulation of PCr in DII embryos indicates a positive energy balance and is consistent with previous reports of high ATP/ADP ratios during diapause (48). The decline in PCr and subsequent rise in creatine in post-DII embryos suggests that ATP demand is outpacing ATP production. This may suggest that aerial exposure is a metabolic stress for post-DII embryos and not for DII embryos. In addition to its role in buffering cellular ATP levels, creatine and PCr have been shown to exhibit a number of cytoprotective effects associated with membranes including: stabilization, alteration of phase transition temperature, and reduction of leak (62). Additionally, PCr can have protective effects against ischemic injury (26, 56). Thus, the accumulation of PCr in DII embryos may offer protective effects that contribute to their much higher tolerance of aerial dehydration stress compared to post-DII embryos.

Glutamate Metabolism. Gamma-aminobutyrate (GABA) is accumulated in both DII (1.6-fold) and post-DII embryos (20-fold) during long-term exposures (Fig 3; Supplemental Table S5). GABA is known to accumulate during anoxia in embryos of *A. limnaeus* and blocking GABA production reduces anoxic survival (51, 75). When GABA is measured spectrophotometrically, it is often undetectable during normal *A. limnaeus* development (75). Thus, the amount of GABA accumulating during dehydration stress probably represents micromolar quantities, and not millimolar levels as seen during anoxia (75). GABA is known to have neuroprotective roles in organisms (21, 36), and is also important in reducing ROS production and protecting against oxidative stress in yeast

(7). Although the levels are likely lower than during anoxia, GABA may still have an important role as a neuroprotective and antioxidant agent during exposures to dehydration.

Carbohydrate

Glycolysis, Gluconeogenesis, and Pyruvate Metabolism and the Pentose Phosphate Pathways. There were 4 metabolites from these pathways that increased in both DII and post-DII embryos: Glucose-6-phosphate, pyruvate, lactate, and sedoheptulose-7-phosphate (Figs 3,7). There were also two stage-specific metabolites that accumulated: glycerate in DII, and phosphoenolpyruvate (PEP) in post-DII embryos (Fig 7; Supplemental Tables S2–4). We previously hypothesized that aerial dehydration stress would limit gas exchange with the environment in concert with the observed decrease in evaporative water loss (46) and lead to self-imposed hypoxia or anoxia. The large increase in GABA and lactate in post-DII embryos supports this hypothesis. Further, the relatively small fold-change in lactate and GABA for DII embryos is consistent with their increase in oxygen consumption in response to aerial dehydration stress (74). Thus, these metabolomics data are consistent with hypoxic metabolism in post-DII but not DII embryos during long-term dehydration stress. Interestingly, the increase in lactate resembles that of the Warburg effect, which is commonly observed in many cancer cells, where enhanced glycolysis and lactate fermentation occur even in the presence of sufficient oxygen. Relying partially on anaerobic mechanisms may offset the reliance on aerobic metabolism which can ultimately lead to increases in ROS. Additionally, lactate in appropriate amounts has been shown to help regulate gene expression through inhibition of histone deacetylase activity and post-translational modifications of histones, act in a neuroprotective role by preventing excitotoxic cell death, and promote oxidative stress resistance (3, 27, 61, 77). Thus, aerobic accumulation of lactate may help fuel a response to dehydration stress through a variety of mechanisms outside of its role in the maintenance of cytoplasmic redox balance.

The accumulation of glucose-6-phosphate and sedoheptulose-7-phosphate (S7P) is consistent with activation of the pentose phosphate pathway (PPP; Fig 7) (41). Shunting of carbon into the PPP results in the production of NADPH used to support

anabolic processes, and also critical for the regeneration of reduced glutathione (33, 41). Accumulation of S7P, but not glyceraldehyde-3-phosphate (G3P) suggests that the oxidative portion of the PPP is used to produce NADPH, but not all of the carbon is shuttled back into glycolysis and instead is allowed to accumulate as S7P. In addition, the accumulation of several ribose metabolism intermediates (Fig 3) is also consistent with increased flux through the PPP. This hypothesis provides a mechanism to support antioxidant capacity (see above discussion of glutathione) while allowing limited immediate carbon flow through glycolysis in the form of G3P, and accumulating a source of carbon (S7P) that could be readily utilized by glycolysis at a later time. These data suggest a critical role for the PPP in supporting aerial dehydration stress in *A. limnaeus* embryos.

Lipids

Fatty Acid, Dicarboxylate. Seven metabolites increased following long-term dehydration: Glutarate (C5-DC), 3-methylglutarate/2-methylglutarate, 2-hydroxyglutarate, adipate (C6-DC), 3-hydroxyadipate, maleate, and sebacate (C10-DC) (Fig 3). Of interest is the accumulation of 2-hydroxyglutarate (2-HG), a molecule known to be produced during hypoxia and a known oncometabolite (23, 37, 66) that can inhibit alpha-ketoglutarate-dependent enzymes involved in many biological processes (73). TET enzymes (DNA demethylases) and histone demethylases are inhibited by 2-HG which can lead to changes in the epigenetic landscape of cells and large-scale changes in gene expression (10, 24, 73). There are several routes for production of 2-HG, including through ‘promiscuous’ reduction of alpha-ketoglutarate by lactate dehydrogenase and malate dehydrogenase (23, 24). Further, 2-HG has been shown to inhibit ATP synthase activity and extend lifespan of *Caenorhabditis elegans* (15) suggesting this molecule could have a number of beneficial effects on *A. limnaeus* embryos during dehydration stress due to aerial incubation.

Fatty Acid, Acyl carnitine. Several acyl carnitine metabolites (*N* = 5) were upregulated: arachidoylcarnitine (C20), arachidonoylcarnitine (C20:4), docosapentaenoylcarnitine (C22:5n6), stearoylcarnitine (C18), palmitoleoylcarnitine (C16:1) (Fig 3). Acyl carnitines

play an essential role in regulating the balance of intracellular sugar and lipid metabolism (28) primarily as carriers for long-chain fatty acids into mitochondria to support β-oxidation (28, 60). Accumulation of these metabolites may suggest reduced mitochondrial fatty acid metabolism during aerial incubation.

*Phospholipid*s. The only metabolite in the phospholipid subpathway to be accumulated in both DII and post-DII embryos was cytidine 5'-diphosphocholine (Fig 3). Cytidine 5'-diphosphocholine is an intermediate product of phosphatidylcholine synthesis. The compound has been used extensively in clinical settings to treat patients with neurological disorders, including cerebral ischemia. The main protective role of cytidine 5'-diphosphocholine is through membrane stabilization (78). Further research has shown cytidine 5'-diphosphocholine protects rat livers from ischemia and reperfusion injury, thus preserving mitochondrial function and reducing oxidative stress (76). Stabilization of cell membranes and reduction of free radical generation may be beneficial to survival of *A. limnaeus* embryos during aerial dehydration stress.

Bile Acid Metabolism. Both taurolithocholate and taurochenodeoxycholate accumulate during long-term exposures (Fig 3). Taurolithocholate accumulates to higher levels in DII embryos (almost 10-fold), while taurochenodeoxycholate exhibits an over 100-fold increase in post-DII embryos. In general, bile acids are toxic due to their ability to act as detergents, but the tauro-derivatives of bile acids tend to be less toxic (55). It is interesting that DII embryos accumulate bile acids despite the absence of liver tissue. In addition to their role in digestion, bile acids can act as signaling molecules via a variety of pathways, including the regulation of a number of nuclear receptors (20). It is possible that these potentially toxic compounds are produced to activate signaling pathways that help support survival. This possibility is intriguing and warrants further investigation.

Cofactors and Vitamins

Nicotinate and Nicotinamide metabolism. Metabolites linked to *de novo* and salvage (nicotinamide, nicotinamide riboside, nicotinamide ribonucleotide, and nicotinate)

pathways of NAD+ synthesis were found to be significantly altered in response to aerial exposure in both DII and post-DII embryos (Fig 8). One difference between DII and post-DII embryos was the significant accumulation of nicotinamide adenine dinucleotide (NAD+) in DII embryos (Fig 8; 17-fold increase). NAD+ is a coenzyme that plays a vital role in redox reactions associated with glycolysis, the TCA cycle, and oxidative phosphorylation. Increasing NAD+ levels in mammals has been linked to improved mitochondrial function under stress (6, 8). Enhancing NAD+ availability in *C. elegans* has been shown to increase lifespan and protect against ROS (34). Conversely, reduction in NAD+ levels is an indication of senescence, as seen in various animal cell lines (16, 34). There is an initial rise in quinolinate in DII embryos followed by a decrease after long-term exposure. It is likely that the decrease in quinolinate contributed to the increase in NAD+ via *de novo* synthesis (Fig 8). The overall rise in NAD+ in DII embryos and maintained levels in post-DII embryos following long-term dehydration stress suggest changes in both demand and synthesis. The accumulation of NAD+ in DII suggests an available pool of NAD+ to contribute to metabolism, while the static levels of NAD+ in post-DII embryos suggests supply and demand are in synergy. The rise in the associated metabolites in the pathway provide a molecular supply for further synthesis of NAD+ via the salvage pathway.

Xenobiotics

Xenobiotics refer to compounds not expected to be present within an organism. There were several metabolites that accumulated which are traditionally thought to be produced by animal microbiomes including: 3 tyrosine metabolites (phenol sulfate, 4-hydroxyphenylpyruvate, and 3-methoxytyrosine) and 3 benzoate metabolites (hippurate, guaiacol sulfate, p-cresol sulfate). Both DII and post-DII embryos exhibited an over 50-fold increase in phenol-sulfate following long-term exposures and hippurate increased over 100-fold in DII embryos (Fig 3). Of these metabolites, hippurate and p-cresol sulfate are known markers for microbiome diversity (40). Hippurate, along with other benzoates, has been shown to inhibit the growth of tumors in mouse cell lines (58). The accumulation of these metabolites in *A. limnaeus* is interesting and may suggest a maternally packaged microbiome in these embryos. While it is possible that these

compounds accumulate due to microbial growth on the surface of the embryos, this is unlikely given the use of antibiotics in the medium, the detection of these metabolites at t = 0, and the lack of other more general microbially-derived compounds that would be expected to accumulate. Interestingly, there is evidence of specific enzymes in the yolk sacs of chicken and tortoise embryos that are capable of producing metabolites that otherwise only exist in microorganisms and plants (9). For example, chicken embryos synthesize lanthionine via enzymes exclusively found in yolk sac endodermal cells. These enzymes disappear upon hatching, which may help explain the lack of lanthionine references in the literature. Alternatively, it is possible that these metabolites are produced by a yolk sac specific microbiome that aids in survival of dehydration stress. Further research needs to be done to elucidate the location, origin, and role of these metabolites in *A. limnaeus* embryos.

Conclusions and Future Directions

The goal of this metabolic profiling study was to gain insight into the biochemical pathways facilitating survival of aerial dehydration stress in *A. limnaeus* embryos. There is evidence of a robust metabolic response to aerial dehydration stress even in metabolically dormant embryos. Evidence exists for a progressive imposition of hypoxia in long-term responses to aerial dehydration stress in post-DII embryos but not during diapause. However, further studies need to be done to delineate whether the responses seen in the post-DII embryos are developmental differences or dehydration-specific responses. In general, amino acid and lipid metabolism appear to play central roles in metabolic adjustments during aerial dehydration stress, and it is clear that embryos are not solely relying on carbohydrate reserves to fuel metabolism. Increased capacity for detoxification of ROS and maintenance of redox balance appear to be of major importance to supporting development and surviving under aerial dehydration stress. It is also interesting that several accumulated metabolites have previously been identified as neuroprotectants. This work offers a first glimpse into the metabolic programs that may support survival of long-term aerial dehydration stress in embryos of *A. limnaeus* that can be functionally tested using genetic and pharmacological approaches.

Perspectives

Embryos of *A. limnaeus* likely spend many months, the preponderance of their life span, aerially incubated in the wild. During aerial exposure, there are a number of metabolites accumulated that are usually associated with waste or have the potential to be toxic (e.g., bile acids, hippurate, lanthionine). Many of these compounds contain nitrogen or other typical waste products of metabolism that are excreted in the urine and feces. When exposed to aerial conditions, embryos of annual killifish must presumably rely on detoxification or compartmentalization of waste product metabolites to ensure the developing embryo remains unharmed. One possible compartment for storage of waste products is the yolk. It is possible that metabolites are being shuttled into the yolk to protect the developing tissues, as seen with sequestration of ammonia in the yolk sac of rainbow trout (59). In amniotic eggs, the eggs of terrestrial vertebrates, waste is transported from the developing embryo into extraembryonic compartments, notably the amnionic, and the allantoic fluid (1, 32, 67). In the anamniotic eggs of fish, waste products such as ammonia or bile acids can be relatively easily lost due to diffusion into the perivitelline fluid during early development, and excretion during late development as the chorion is not a substantial barrier for diffusion of relatively small metabolites (72). However, in *A. limnaeus* the perivitelline fluid is quickly lost during aerial exposures and can no longer function as a mechanism for diffusive loss of metabolic waste products. Indeed, the embryos of annual killifish embryos exposed to aerial incubation have several unique features that approximate the functions of the shell and extraembryonic components of the amniotic eggs of terrestrial species. First, the egg envelope of annual killifish lacks pores, is substantially thicker than in most species of fish, and may serve a physical role in protection of embryos encased in dry mud (57). Second, the enveloping cell layer of annual killifish embryos does not contribute to the skin of the developing embryos as it does in most fishes, instead it forms a syncytial membrane that surrounds the embryo and is shed upon hatching (69). This membrane constitutes the major permeability barrier between the embryo and its environment and has a unique structure with few embedded proteins (25) and an extremely low permeability to water and salts (29). The enveloping layer in annual killifishes effectively creates an extra-embryonic membrane-bound compartment that surrounds and protects

the embryo in a manner similar to an amniotic chamber in terrestrial eggs. Thus, it is possible that a number of the compounds that are typically excreted as waste may be stored in either the yolk sac, or in extraembryonic fluid bound by the enveloping cell layer. In fact, many of the accumulated compounds identified in this study are known components of amniotic and allantoic fluid in other species (1, 32, 67) and may suggest a unique extraembryonic compartment in annual killifish embryos. Further exploration into the localization of these metabolites will help elucidate their possible function during survival of dehydration stress due to aerial incubation.

Acknowledgements

We would like to thank all of the undergraduate student workers who helped with animal husbandry and maintenance.

Grants

The work was supported by National Science Foundation grant IOS-1354549 to JEP.

Disclosures

The authors declare no competing interests.

References

1. **Aktuğ T, Uçan B, Olguner M, Akgür F, Özer E, Calişkan S, and Önvural B**. Amnio-allantoic fluid exchange for the prevention of intestinal damage in gastroschisis III: determination of the waste products removed by exchange. *European journal of pediatric surgery* 8: 326-328, 1998.
2. **Bachhawat AK, and Yadav S**. The glutathione cycle: Glutathione metabolism beyond the γ-glutamyl cycle. *IUBMB life* 70: 585-592, 2018.
3. **Berthet C, Lei H, Thevenet J, Gruetter R, Magistretti PJ, and Hirt L**. Neuroprotective role of lactate after cerebral ischemia. *Journal of Cerebral Blood Flow & Metabolism* 29: 1780-1789, 2009.
4. **Blackstone E, Morrison M, and Roth MB**. H_2S induces a suspended animation-like state in mice. *Science* 308: 518, 2005.
5. **Bosco MC, Rapisarda A, Massazza S, Melillo G, Young H, and Varesio L**. The tryptophan catabolite picolinic acid selectively induces the chemokines macrophage inflammatory protein-1α and-1β in macrophages. *The Journal of Immunology* 164: 3283-3291, 2000.
6. **Canto C, Menzies KJ, and Auwerx J**. NAD+ metabolism and the control of energy homeostasis: a balancing act between mitochondria and the nucleus. *Cell metabolism* 22: 31-53, 2015.
7. **Cao J, Barbosa JM, Singh NK, and Locy RD**. GABA shunt mediates thermotolerance in *Saccharomyces cerevisiae* by reducing reactive oxygen production. *Yeast* 30: 129-144, 2013.
8. **Cerutti R, Pirinen E, Lamperti C, Marchet S, Sauve AA, Li W, Leoni V, Schon EA, Dantzer F, and Auwerx J**. NAD+-dependent activation of Sirt1 corrects the phenotype in a mouse model of mitochondrial disease. *Cell metabolism* 19: 1042-1049, 2014.
9. **Chapeville F, and Fromageot P**. “Vestigial” enzymes during embryonic development. *Advances in Enzyme Regulation* 5: 155-158, 1967.
10. **Charitou P, Rodriguez-Colman M, Gerrits J, van Triest M, Koerkamp MG, Hornsveld M, Holstege F, Verhoeven-Duif NM, and Burgering BM**. FOXOs support the metabolic requirements of normal and tumor cells by promoting IDH1 expression. *EMBO Reports* 16: 456-466, 2015.
11. **Elrod JW, Calvert JW, Morrison J, Doeller JE, Kraus DW, Tao L, Jiao X, Scalia R, Kiss L, and Szabo C**. Hydrogen sulfide attenuates myocardial ischemia-reperfusion injury by preservation of mitochondrial function. *Proceedings of the National Academy of Sciences of the United States of America* 104: 15560-15565, 2007.
12. **Ernst V, Levin DH, and London IM**. Inhibition of protein synthesis initiation by oxidized glutathione: activation of a protein kinase that phosphorylates the α subunit of eukaryotic initiation factor 2. *Proceedings of the National Academy of Sciences of the United States of America* 75: 4110-4114, 1978.
13. **Fontana M, Ricci G, Solinas S, Antonucci A, Serao I, Dupre S, and Cavallini D**. [^{35}S] Lanthionine ketimine binding to bovine brain membranes. *Biochemical and biophysical research communications* 171: 480-486, 1990.

14. **França M, Panek A, and Eleutherio E**. Oxidative stress and its effects during dehydration. *Comparative Biochemistry and Physiology Part A: Molecular & Integrative Physiology* 146: 621-631, 2007.
15. **Fu X, Chin RM, Vergnes L, Hwang H, Deng G, Xing Y, Pai MY, Li S, Ta L, and Fazlollahi F**. 2-Hydroxyglutarate inhibits ATP synthase and mTOR signaling. *Cell Metabolism* 22: 508-515, 2015.
16. **Gomes AP, Price NL, Ling AJ, Moslehi JJ, Montgomery MK, Rajman L, White JP, Teodoro JS, Wrann CD, and Hubbard BP**. Declining NAD+ induces a pseudohypoxic state disrupting nuclear-mitochondrial communication during aging. *Cell* 155: 1624-1638, 2013.
17. **Grant R, Coggan S, and Smythe G**. The physiological action of picolinic acid in the human brain. *International Journal of Tryptophan Research* 2: IJTR-S2469, 2009.
18. **Hansen JM, Go Y-M, and Jones DP**. Nuclear and mitochondrial compartmentation of oxidative stress and redox signaling. *Annual Review of Pharmacology and Toxicology* 46: 215-234, 2006.
19. **Hensley K, Venkova K, and Christov A**. Emerging biological importance of central nervous system lanthionines. *Molecules* 15: 5581-5594, 2010.
20. **Hylemon PB, Zhou H, Pandak WM, Ren S, Gil G, and Dent P**. Bile acids as regulatory molecules. *Journal of Lipid Research* 50: 1509-1520, 2009.
21. **Hylland P, and Nilsson GE**. Extracellular levels of amino acid neurotransmitters during anoxia and forced energy deficiency in crucian carp brain. *Brain research* 823: 49-58, 1999.
22. **Inoue M**. Glutathionists in the battlefield of gamma-glutamyl cycle. *Archives of biochemistry and biophysics* 595: 61-63, 2016.
23. **Intlekofer AM, Dematteo RG, Venneti S, Finley LW, Lu C, Judkins AR, Rustenburg AS, Grinaway PB, Chodera JD, and Cross JR**. Hypoxia induces production of L-2-hydroxyglutarate. *Cell metabolism* 22: 304-311, 2015.
24. **Intlekofer AM, Wang B, Liu H, Shah H, Carmona-Fontaine C, Rustenburg AS, Salah S, Gunner MR, Chodera JD, and Cross JR**. L-2-Hydroxyglutarate production arises from noncanonical enzyme function at acidic pH. *Nature chemical biology* 13: 494, 2017.
25. **Jorgenson N-C, and Schmalbruch H**. The eggs of the freshwater fish *Epiplatys dageti* have tight plasma membranes without intramembranous particles. *Cell and Tissue Research* 235: 643-646, 1984.
26. **Landoni G, Zangrillo A, Lomivorotov VV, Likhvantsev V, Ma J, De Simone F, and Fominskiy E**. Cardiac protection with phosphocreatine: a meta-analysis. *Interactive Cardiovascular and Thoracic Surgery* 23: 637-646, 2016.
27. **Latham T, Mackay L, Sproul D, Karim M, Culley J, Harrison DJ, Hayward L, Langridge-Smith P, Gilbert N, and Ramsahoye BH**. Lactate, a product of glycolytic metabolism, inhibits histone deacetylase activity and promotes changes in gene expression. *Nucleic Acids Research* 40: 4794-4803, 2012.
28. **Li S, Gao D, and Jiang Y**. Function, detection and alteration of acylcarnitine metabolism in hepatocellular carcinoma. *Metabolites* 9: 36, 2019.
29. **Machado BE, and Podrabsky JE**. Salinity tolerance in diapausing embryos of the annual killifish *Austrofundulus limnaeus* is supported by exceptionally low water and

ion permeability. *Journal of Comparative Physiology B: Biochemical, Systemic, and Environmental Physiology* 177: 809-820, 2007.
30. **Masella R, Di Benedetto R, Varì R, Filesi C, and Giovannini C**. Novel mechanisms of natural antioxidant compounds in biological systems: involvement of glutathione and glutathione-related enzymes. *Journal of Nutritional Biochemistry* 16: 577-586, 2005.
31. **Meller CL, Meller R, Simon RP, Culpepper KM, and Podrabsky JE**. Cell cycle arrest associated with anoxia-induced quiescence, anoxic preconditioning, and embryonic diapause in embryos of the annual killifish *Austrofundulus limnaeus*. *Journal of Comparative Physiology B* 182: 909-920, 2012.
32. **Mellor D, and Slater J**. Daily changes in amniotic and allantoic fluid during the last three months of pregnancy in conscious, unstressed ewes, with catheters in their foetal fluid sacs. *The Journal of Physiology* 217: 573-604, 1971.
33. **Minard KI, and McAlister-Henn L**. Antioxidant function of cytosolic sources of NADPH in yeast. *Free Radical Biology and Medicine* 31: 832-843, 2001.
34. **Mouchiroud L, Houtkooper RH, Moullan N, Katsyuba E, Ryu D, Cantó C, Mottis A, Jo Y-S, Viswanathan M, and Schoonjans K**. The NAD+/sirtuin pathway modulates longevity through activation of mitochondrial UPR and FOXO signaling. *Cell* 154: 430-441, 2013.
35. **Nada SE, Tulsulkar J, Raghavan A, Hensley K, and Shah ZA**. A derivative of the CRMP2 binding compound lanthionine ketimine provides neuroprotection in a mouse model of cerebral ischemia. *Neurochemistry international* 61: 1357-1363, 2012.
36. **Nilsson GE, Lutz PL, and Jackson TL**. Neurotransmitters and anoxic survival of the brain: A comparison of anoxia-tolerant and anoxia-intolerant vertebrates. *Physiological Zoology* 64: 638-652, 1991.
37. **Oldham WM, Clish CB, Yang Y, and Loscalzo J**. Hypoxia-mediated increases in L-2-hydroxyglutarate coordinate the metabolic response to reductive stress. *Cell metabolism* 22: 291-303, 2015.
38. **Olson KR**. H_2S and polysulfide metabolism: conventional and unconventional pathways. *Biochemical Pharmacology* 149: 77-90, 2018.
39. **Orlowski M, and Meister A**. The γ-glutamyl cycle: a possible transport system for amino acids. *Proceedings of the National Academy of Sciences of the United States of America* 67: 1248-1255, 1970.
40. **Pallister T, Jackson MA, Martin TC, Zierer J, Jennings A, Mohney RP, MacGregor A, Steves CJ, Cassidy A, and Spector TD**. Hippurate as a metabolomic marker of gut microbiome diversity: modulation by diet and relationship to metabolic syndrome. *Scientific reports* 7: 1-9, 2017.
41. **Patra KC, and Hay N**. The pentose phosphate pathway and cancer. *Trends in Biochemical Sciences* 39: 347-354, 2014.
42. **Perna AF, Anishchenko E, Vigorito C, Zacchia M, Trepiccione F, D'Aniello S, and Ingrosso D**. Zebrafish, a novel model system to study uremic toxins: the case for the sulfur amino acid lanthionine. *International journal of molecular sciences* 19: 1323, 2018.
43. **Podrabsky J, Riggs C, Romney A, Woll S, Wagner J, Culpepper K, and Cleaver T**. Embryonic development of the annual killifish *Austrofundulus limnaeus*: An

742 emerging model for ecological and evolutionary developmental biology research and
743 instruction. *Developmental Dynamics* 246: 779-801, 2017.
744 44. **Podrabsky J, Riggs C, and Wagner J**. Tolerance of Environmental Stress. In:
745 *Annual Fishes Life History Strategy, Diversity, and Evolution*, edited by Berois N, García
746 G, and De Sá R. Boca Raton, FL USA: CRC Press, Taylor & Francis, 2016, p. 159-184.
747 45. **Podrabsky JE**. Husbandry of the annual killifish *Austrofundulus limnaeus* with
748 special emphasis on the collection and rearing of embryos. *Environmental Biology of*
749 *Fishes* 54: 421-431, 1999.
750 46. **Podrabsky JE, Carpenter JF, and Hand SC**. Survival of water stress in annual
751 fish embryos: dehydration avoidance and egg envelope amyloid fibers. *American*
752 *Journal of Physiology* 280: R123-R131, 2001.
753 47. **Podrabsky JE, Garrett IDF, and Kohl ZF**. Alternative developmental pathways
754 associated with diapause regulated by temperature and maternal influences in embryos
755 of the annual killifish *Austrofundulus limnaeus*. *Journal of Experimental Biology* 213:
756 3280-3288, 2010.
757 48. **Podrabsky JE, and Hand SC**. The bioenergetics of embryonic diapause in an
758 annual killifish, *Austrofundulus limnaeus*. *Journal of Experimental Biology* 202: 2567-
759 2580, 1999.
760 49. **Podrabsky JE, and Hand SC**. Depression of protein synthesis during diapause
761 in embryos of the annual killifish *Austrofundulus limnaeus*. *Physiological and*
762 *Biochemical Zoology* 73: 799-808, 2000.
763 50. **Podrabsky JE, Hrbek T, and Hand SC**. Physical and chemical characteristics of
764 ephemeral pond habitats in the Maracaibo basin and Llanos region of Venezuela.
765 *Hydrobiologia* 362: 67-78, 1998.
766 51. **Podrabsky JE, Lopez JP, Fan TWM, Higashi R, and Somero GN**. Extreme
767 anoxia tolerance in embryos of the annual killifish *Austrofundulus limnaeus*: Insights
768 from a metabolomics analysis. *Journal of Experimental Biology* 210: 2253-2266, 2007.
769 52. **Polačik M, and Podrabsky JE**. Temporary Environments. In: *Extremophile*
770 *Fishes: Ecology, Evolution, and Physiology of Teleosts in Extreme Environments*, edited
771 by Riesch R, Tobler M, and Plath M. Cham, Switzerland: Springer, 2015, p. 217-245.
772 53. **Polačik M, Vrtílek M, Reichard M, Blazek R, and Podrabsky J**. Embryo
773 ecology: A critical role of environment in the diapause of wild annual fish populations.
774 *Freshwater Biology* submitted: 2020.
775 54. **Romney A, Davis E, Corona M, Wagner J, and Podrabsky J**. Temperature
776 dependent vitamin D signaling regulates developmental trajectory associated with
777 diapause in an annual killifish. *Proceedings of the National Academy of Sciences of the*
778 *United States of America* 115: 12763-12768, 2018.
779 55. **Rust C, Karnitz LM, Paya CV, Moscat J, Simari RD, and Gores GJ**. The bile
780 acid taurochenodeoxycholate activates a phosphatidylinositol 3-kinase-dependent
781 survival signaling cascade. *Journal of Biological Chemistry* 275: 20210-20216, 2000.
782 56. **Saks V, and Strumia E**. Phosphocreatine: molecular and cellular aspects of the
783 mechanism of cardioprotective action. *Current Therapeutic Research* 53: 565-598,
784 1993.
785 57. **Schoots AFM, Stikkelbroeck JJM, Bekhuis JF, and Denuce JM**. Hatching in
786 teleostean fishes: fine structural changes in the egg envelope during enzymatic
787 breakdown *in vivo* and *in vitro*. *Journal of Ultrastructure Research* 80: 185-196, 1982.

58. **Spustova V, and Oravec C**. Antitumor effect of hippurate. An experimental study using various mouse tumor strains. *Neoplasma* 36: 317-320, 1989.
59. **Steele SL, Chadwick TD, and Wright PA**. Ammonia detoxification and localization of urea cycle enzyme activity in embryos of the rainbow trout (*Oncorhynchus mykiss*) in relation to early tolerance to high environmental ammonia levels. *Journal of Experimental Biology* 204: 2145-2154, 2001.
60. **Tarasenko TN, Cusmano-Ozog K, and McGuire PJ**. Tissue acylcarnitine status in a mouse model of mitochondrial β-oxidation deficiency during metabolic decompensation due to influenza virus infection. *Molecular Genetics and Metabolism* 125: 144-152, 2018.
61. **Tauffenberger A, Fiumelli H, Almustafa S, and Magistretti PJ**. Lactate and pyruvate promote oxidative stress resistance through hormetic ROS signaling. *Cell Death & Disease* 10: 1-16, 2019.
62. **Tokarska-Schlattner M, Epand RF, Meiler F, Zandomeneghi G, Neumann D, Widmer HR, Meier BH, Epand RM, Saks V, and Wallimann T**. Phosphocreatine interacts with phospholipids, affects membrane properties and exerts membrane-protective effects. *PLoS One* 7: 2012.
63. **Vigorito C, Anishchenko E, Mele L, Capolongo G, Trepiccione F, Zacchia M, Lombari P, Capasso R, Ingrosso D, and Perna AF**. Uremic toxin lanthionine interferes with the transsulfuration pathway, angiogenetic signaling and increases intracellular calcium. *International journal of molecular sciences* 20: 2269, 2019.
64. **Wagner J, Singh P, Romney A, Riggs C, Minx P, Woll S, Roush J, Warren W, Brunet A, and Podrabsky J**. The genome of *Austrofundulus limnaeus* offers insights into extreme vertebrate stress tolerance and embryonic development. *BMC Genomics* 19: 155, 2018.
65. **Wagner JT, Knapp MJ, and Podrabsky JE**. Antioxidant capacity and anoxia tolerance in *Austrofundulus limnaeus* embryos. *Journal of Experimental Biology* 222: jeb204347, 2019.
66. **Ward PS, Patel J, Wise DR, Abdel-Wahab O, Bennett BD, Coller HA, Cross JR, Fantin VR, Hedvat CV, and Perl AE**. The common feature of leukemia-associated IDH1 and IDH2 mutations is a neomorphic enzyme activity converting α-ketoglutarate to 2-hydroxyglutarate. *Cancer Cell* 17: 225-234, 2010.
67. **Williams M, Wallace S, Tyler J, McCall C, Gutierrez A, and Spano J**. Biochemical characteristics of amniotic and allantoic fluid in late gestational mares. *Theriogenology* 40: 1251-1257, 1993.
68. **Winston PW, and Bates DH**. Saturated solutions for the control of humidity in biological research. *Ecology* 41: 232-237, 1960.
69. **Wourms JP**. The developmental biology of annual fish II. Naturally occuring dispersion and reaggregation of blastomeres during the development of annual fish eggs. *Journal of Experimental Zoology* 182: 169-200, 1972.
70. **Wourms JP**. The developmental biology of annual fishes I. Stages in the normal development of *Austrofundulus myersi* Dahl. *Journal of Experimental Zoology* 182: 143-168, 1972.
71. **Wourms JP**. The developmental biology of annual fishes III. Pre-embryonic and embryonic diapause of variable duration in the eggs of annual fishes. *Journal of Experimental Zoology* 182: 389-414, 1972.

72. **Wright PA, Felskie A, and Anderson PM**. Induction of ornithine-urea cycle enzymes and nitrogen metabolism and excretion in rainbow trout (*Oncorhynchus mykiss*) during early life stages. *Journal of Experimental Biology* 198: 127-135, 1995.
73. **Xu W, Yang H, Liu Y, Yang Y, Wang P, Kim S-H, Ito S, Yang C, Wang P, and Xiao M-T**. Oncometabolite 2-hydroxyglutarate is a competitive inhibitor of α-ketoglutarate-dependent dioxygenases. *Cancer Cell* 19: 17-30, 2011.
74. **Zajic D, Nicholson J, and Podrabsky J**. No water, no problem: Stage-specific metabolic responses to dehydration stress in annual killifish embryos. *Journal of Experimental Biology* Accepted: 2020.
75. **Zajic D, and Podrabsky J**. GABA daba doo, anoxia got nothing on you: GABA metabolism is crucial for long-term survival in annual killifish embryos. *Journal of Experimental Biology* Submitted: 2020.
76. **Zazueta C, Buelna-Chontal M, Macías-López A, Román-Anguiano NG, González-Pacheco H, Pavón N, Springall R, Aranda-Frausto A, Bojalil R, and Silva-Palacios A**. Cytidine-5'-diphosphocholine protects the liver from ischemia/reperfusion injury preserving mitochondrial function and reducing oxidative stress. *Liver Transplantation* 24: 1070-1083, 2018.
77. **Zhang D, Tang Z, Huang H, Zhou G, Cui C, Weng Y, Liu W, Kim S, Lee S, and Perez-Neut M**. Metabolic regulation of gene expression by histone lactylation. *Nature* 574: 575-580, 2019.
78. **Zweifler RM**. Membrane stabilizer: citicoline. *Current Medical Research and Opinion* 18: s14-s17, 2002.

Figure Captions

Figure 1. Schematic of the experimental design and sampling regimen used for metabolomics analysis. Embryos were exposed to 85% relative humidity (RH) at the developmental stage listed (DII or WS 36) for up to 28 d (*N* = 6, each replicate contained 25 embryos). Developmental stage at time of sampling is included below each timepoint. WS, Wourms' stage; DII, diapause II.

Figure 2. Heat maps of fold change from t = 0 of 673 metabolites detected in embryos.
Heat maps (organized by superpathway) represent the $\log_2$ fold change of each metabolite in response to short-term (S) and long-term (L) aerial dehydration stress in diapause II (DII) and post-DII embryos when compared to control embryos at t = 0. Metabolites are clustered by subpathways. Major subpathways are indicated on the left of each heat map. Within each heatmap, fold changes are displayed for all comparisons, even though fold changes may not be statistically significant for all columns. For details on sampling, see Figure 1.

Figure 3. Shared metabolites that significantly change during long-term aerial dehydration stress in DII and post-DII embryos. A total of 18 metabolites decreased and 71 metabolites increased in both stages. Values are $\log_2$ fold changes relative to t = 0. The vertical dotted line separates the downregulated (left) and upregulated (right) metabolites. The color of each metabolite denotes superpathway. Metabolites with asterisks indicate compounds that have not been confirmed based on standards, but Metabolon is confident in their identity.

Figure 4. Indications of altered transsulfuration activity and antioxidant utilization in DII and post-DII embryos. Box plot data illustrating metabolites contributing to methionine, cysteine, and glutathione metabolism. Data (scaled intensity) are presented as box plots with a line drawn at the median (mean indicated by a plus symbol) and the box indicating upper and lower quartiles. Error bars are distribution minimums and

maximums. Vertical dotted lines separate data from DII (blue) and post-DII embryos (orange). Data are organized by aerial exposure treatment (C, control; S, short-term; L, long-term). Asterisks represent metabolites that were significantly different from t = 0 (Welch's two-sample t-test, $P < 0.05$). Raw values for each metabolite were scaled to set the median across all samples to 1 and were normalized to DNA content. Relevant enzymes are included (grey boxes). CBS, cystathionine β-synthase; CSE, cystathionine γ-lyase; GCS, gamma-glutamylcysteine synthetase; GS, glutathione synthase; GGT, gamma-glutamyl transferase.

Figure 5. Changes in gamma-glutamyl amino acid metabolism in DII and post-DII embryos. Box plots illustrating metabolites involved in gamma-glutamyl amino acid metabolism that were significantly altered in at least one stage. For details of box plots and presentation of scaled intensity data, please see the legend of Figure 4. Asterisks represent metabolites that were significantly different from t = 0 (Welch's two-sample t-test, $P < 0.05$). Gamma-glutamylisoleucine (asterisk) had not been confirmed based on a standard, but Metabolon is confident in the identity.

Figure 6. Changes in creatine metabolism in DII and post-DII embryos. Box plots illustrating metabolites involved in creatine metabolism. For details of box plots and presentation of scaled intensity data, please see the legend of Figure 4. Asterisks represent metabolites that were significantly different from t = 0 (Welch's two-sample t-test, $P < 0.05$).

Figure 7. Changes in glycolysis and pentose phosphate pathway metabolism in DII and post-DII embryos. Box plots illustrating metabolites involved in glycolysis and pentose phosphate pathway (PPP) metabolism. For details of box plots and presentation of scaled intensity data, please see the legend of Figure 4. Asterisks represent metabolitrs that were significantly different from t = 0 (Welch's two-sample t-test, $P < 0.05$).

Figure 8. Changes in nicotinate and nicotinamide metabolism in DII and post-DII embryos. Box plots illustrating metabolites contributing to nicotinate and nicotinamide metabolism. For details of box plots and presentation of scaled intensity data, please see the legend of Figure 4. Asterisks represent metabolites that were significantly different from t = 0 (Welch's two-sample t-test, $P < 0.05$).

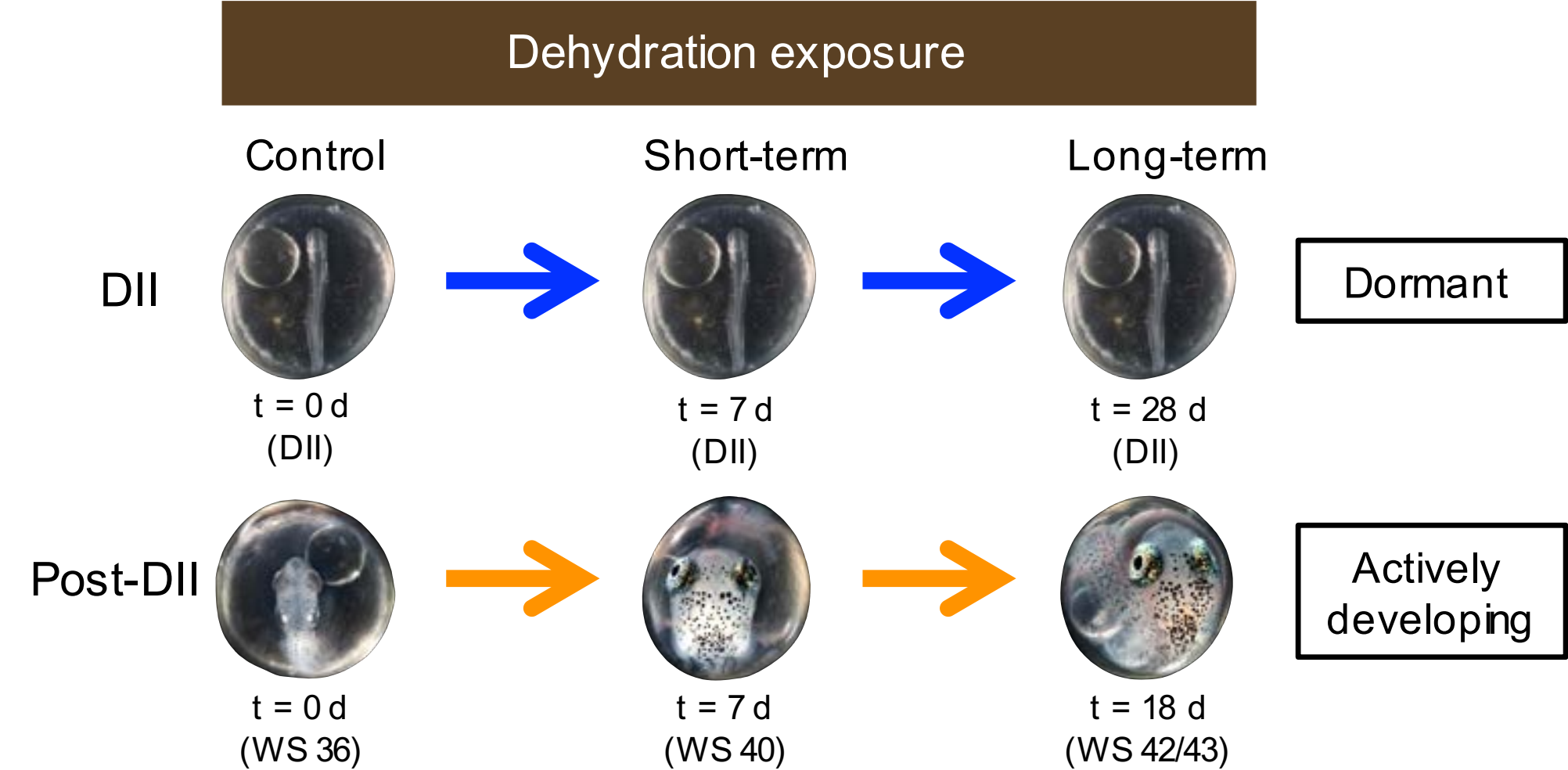
Dehydration exposure
Control
Short-term
Long-term
DII
t = 0 d
(DII)
t = 7 d
(DII)
t = 28 d
(DII)
Dormant
Post-DII
t = 0 d
(WS 36)
t = 7 d
(WS 40)
t = 18 d
(WS 42/43)
Actively developing

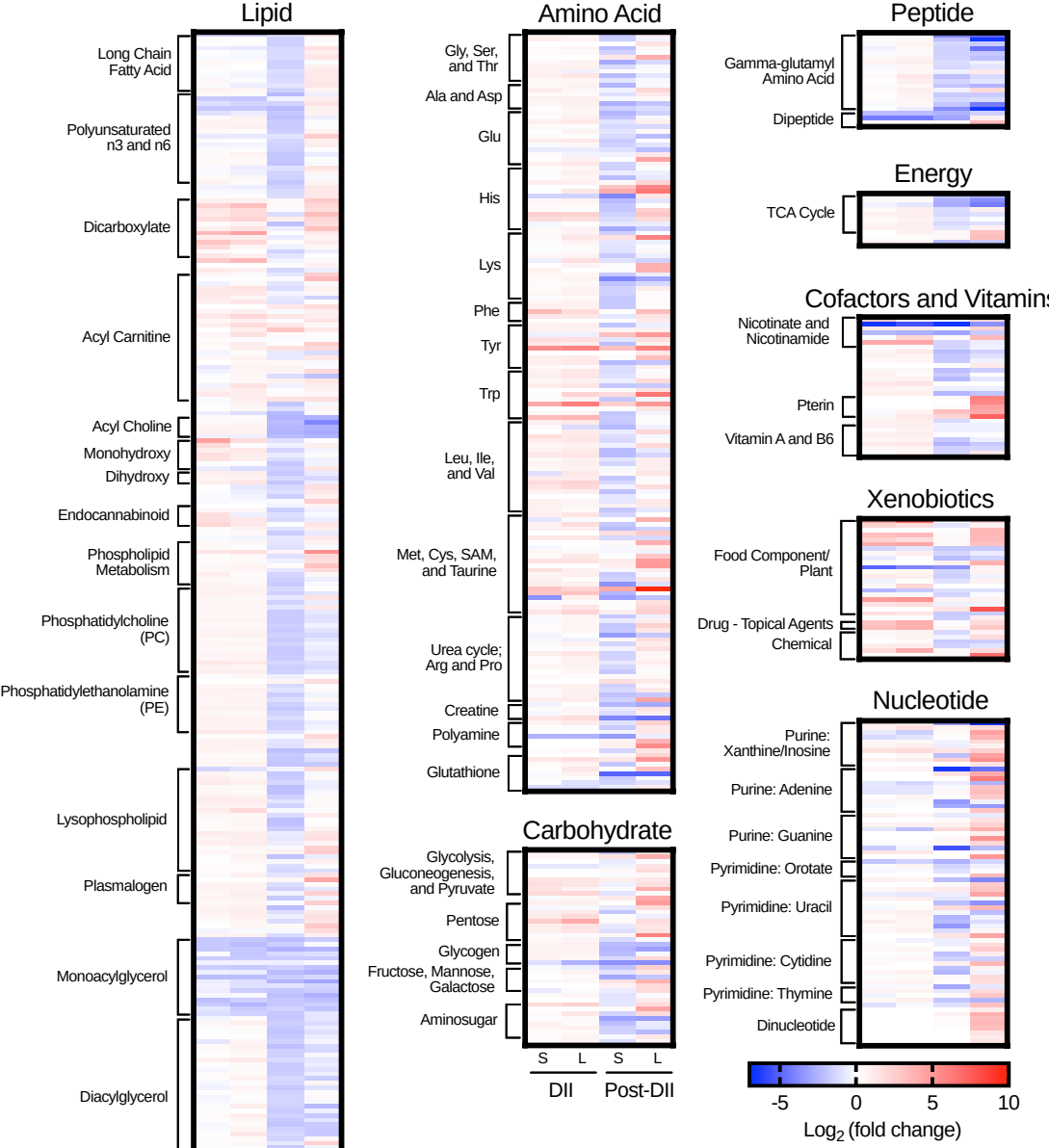
Lipid
Long Chain Fatty Acid
Polyunsaturated n3 and n6
Dicarboxylate
Acyl Carnitine
Acyl Choline
Monohydroxy
Dihydroxy
Endocannabinoid
Phospholipid Metabolism
Phosphatidylcholine (PC)
Phosphatidylethanolamine (PE)
Lysophospholipid
Plasmalogen
Monoacylglycerol
Diacylglycerol
Ceramides
Dihydrosphingomyelins
Sphingomyelins
Sterol
Bile metabolism
Amino Acid
Gly, Ser, and Thr
Ala and Asp
Glu
His
Lys
Phe
Tyr
Trp
Leu, Ile, and Val
Met, Cys, SAM, and Taurine
Urea cycle; Arg and Pro
Creatine
Polyamine
Glutathione
Carbohydrate
Glycolysis, Gluconeogenesis, and Pyruvate
Pentose
Glycogen
Fructose, Mannose, Galactose
Aminosugar
S L S L
DII Post-DII
Peptide
Gamma-glutamyl Amino Acid
Dipeptide
Energy
TCA Cycle
Cofactors and Vitamins
Nicotinate and Nicotinamide
Pterin
Vitamin A and B6
Xenobiotics
Food Component/ Plant
Drug - Topical Agents
Chemical
Nucleotide
Purine: Xanthine/Inosine
Purine: Adenine
Purine: Guanine
Pyrimidine: Orotate
Pyrimidine: Uracil
Pyrimidine: Cytidine
Pyrimidine: Thymine
Dinucleotide
-5 0 5 10
Log2 (fold change)

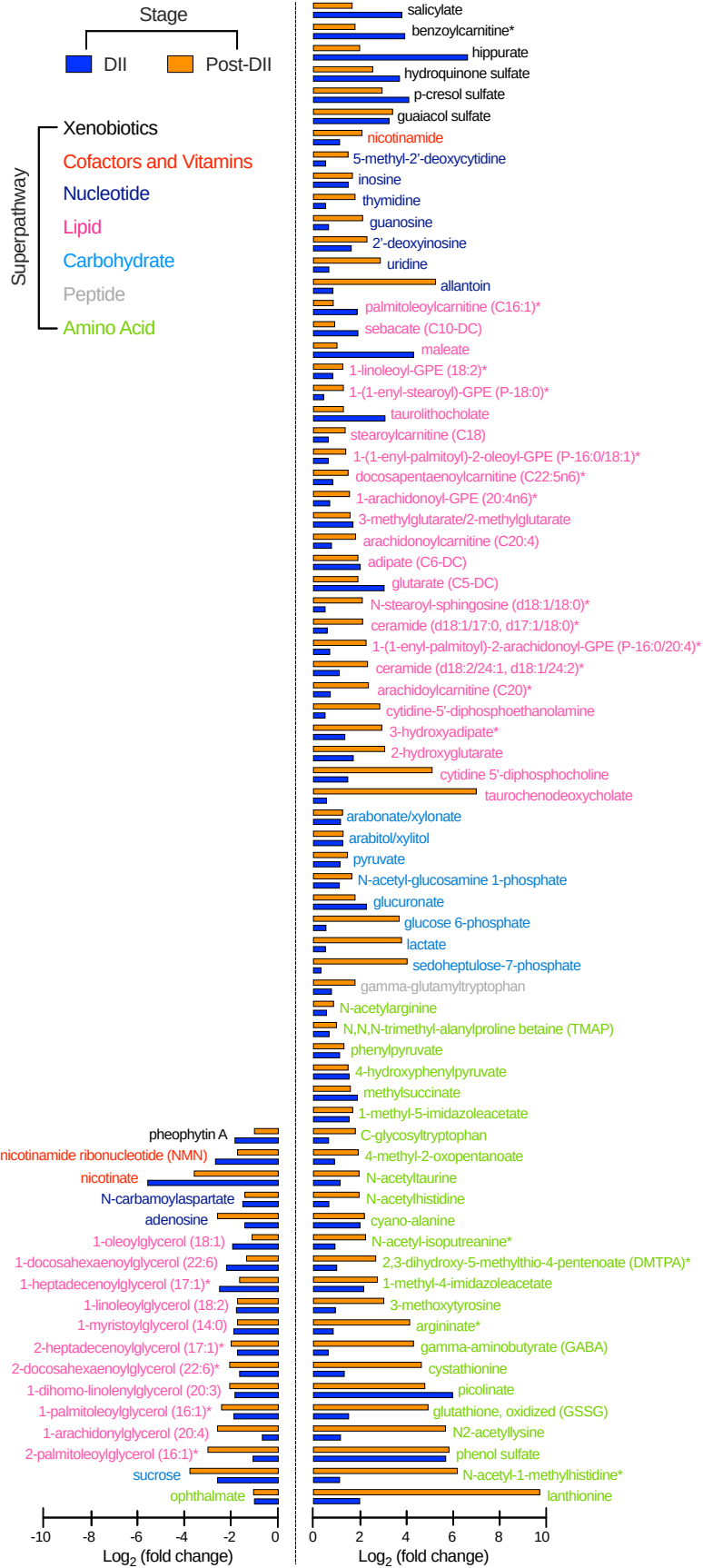
Stage
DII
Post-DII
Superpathway
Xenobiotics
Cofactors and Vitamins
Nucleotide
Lipid
Carbohydrate
Peptide
Amino Acid
salicylate
benzoylcarnitine*
hippurate
hydroquinone sulfate
p-cresol sulfate
guaiacol sulfate
nicotinamide
5-methyl-2'-deoxycytidine
inosine
thymidine
guanosine
2'-deoxyinosine
uridine
allantoin
palmitoleoylcarnitine (C16:1)*
sebacate (C10-DC)
maleate
1-linoleoyl-GPE (18:2)*
1-(1-enyl-stearoyl)-GPE (P-18:0)*
taurolithocholate
stearoylcarnitine (C18)
1-(1-enyl-palmitoyl)-2-oleoyl-GPE (P-16:0/18:1)*
docosapentaenoylcarnitine (C22:5n6)*
1-arachidonoyl-GPE (20:4n6)*
3-methylglutarate/2-methylglutarate
arachidonoylcarnitine (C20:4)
adipate (C6-DC)
glutarate (C5-DC)
N-stearoyl-sphingosine (d18:1/18:0)*
ceramide (d18:1/17:0, d17:1/18:0)*
1-(1-enyl-palmitoyl)-2-arachidonoyl-GPE (P-16:0/20:4)*
ceramide (d18:2/24:1, d18:1/24:2)*
arachidoylcarnitine (C20)*
cytidine-5'-diphosphoethanolamine
3-hydroxyadipate*
2-hydroxyglutarate
cytidine 5'-diphosphocholine
taurochenodeoxycholate
arabonate/xylonate
arabitol/xylitol
pyruvate
N-acetyl-glucosamine 1-phosphate
glucuronate
glucose 6-phosphate
lactate
sedoheptulose-7-phosphate
gamma-glutamyltryptophan
N-acetylarginine
N,N,N-trimethyl-alanylproline betaine (TMAP)
phenylpyruvate
4-hydroxyphenylpyruvate
methylsuccinate
1-methyl-5-imidazoleacetate
C-glycosyltryptophan
4-methyl-2-oxopentanoate
N-acetyltaurine
N-acetylhistidine
cyano-alanine
N-acetyl-isoputreanine*
2,3-dihydroxy-5-methylthio-4-pentenoate (DMTPA)*
1-methyl-4-imidazoleacetate
3-methoxytyrosine
argininate*
gamma-aminobutyrate (GABA)
cystathionine
picolinate
glutathione, oxidized (GSSG)
N2-acetyllysine
phenol sulfate
N-acetyl-1-methylhistidine*
lanthionine
pheophytin A
nicotinamide ribonucleotide (NMN)
nicotinate
N-carbamoylaspartate
adenosine
1-oleoylglycerol (18:1)
1-docosahexaenoylglycerol (22:6)
1-heptadecenoylglycerol (17:1)*
1-linoleoylglycerol (18:2)
1-myristoylglycerol (14:0)
2-heptadecenoylglycerol (17:1)*
2-docosahexaenoylglycerol (22:6)*
1-dihomo-linolenylglycerol (20:3)
1-palmitoleoylglycerol (16:1)*
1-arachidonylglycerol (20:4)
2-palmitoleoylglycerol (16:1)*
sucrose
ophthalmate
-10
-8
-6
-4
-2
0
Log2 (fold change)
0
2
4
6
8
10
Log2 (fold change)

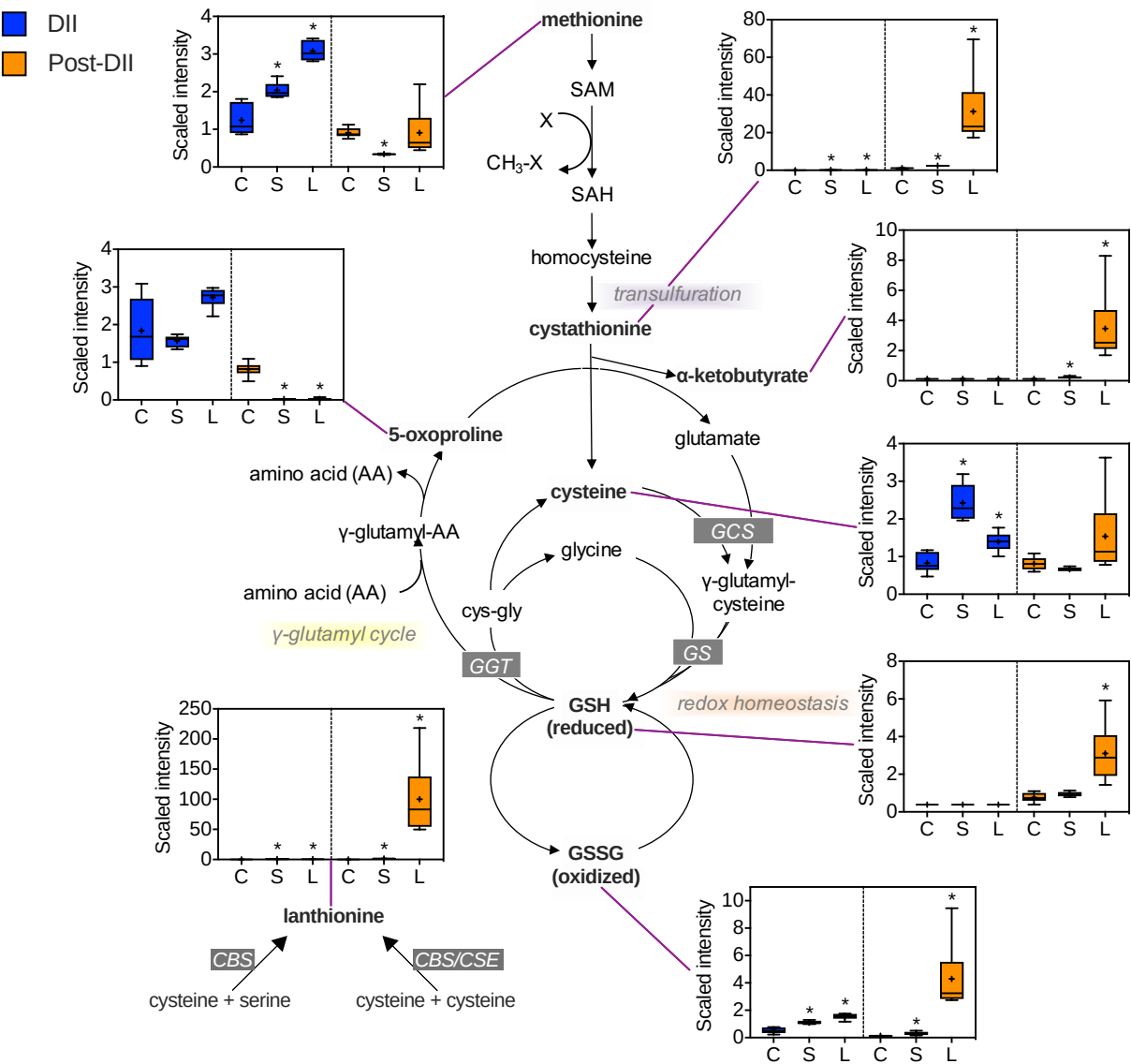
DII
Post-DII
methionine
SAM
X
CH3-X
SAH
homocysteine
transulfuration
cystathionine
α-ketobutyrate
5-oxoproline
glutamate
amino acid (AA)
γ-glutamyl-AA
amino acid (AA)
γ-glutamyl cycle
cysteine
glycine
cys-gly
GCS
γ-glutamyl-cysteine
GGT
GS
GSH (reduced)
redox homeostasis
GSSG (oxidized)
lanthionine
CBS
CBS/CSE
cysteine + serine
cysteine + cysteine
Scaled intensity
C S L C S L

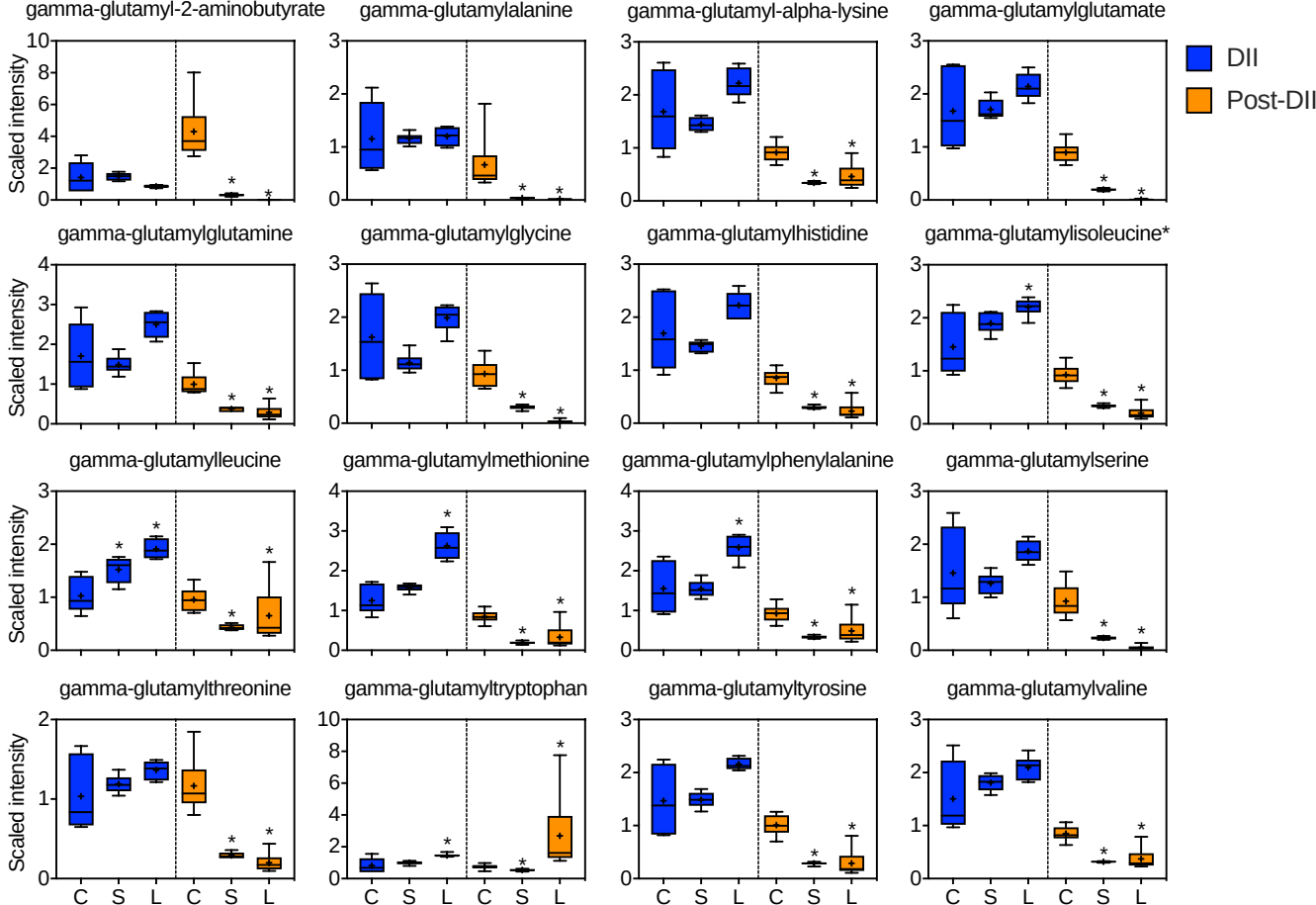
gamma-glutamyl-2-aminobutyrate
gamma-glutamylalanine
gamma-glutamyl-alpha-lysine
gamma-glutamylglutamate
gamma-glutamylglutamine
gamma-glutamylglycine
gamma-glutamylhistidine
gamma-glutamylisoleucine*
gamma-glutamylleucine
gamma-glutamylmethionine
gamma-glutamylphenylalanine
gamma-glutamylserine
gamma-glutamylthreonine
gamma-glutamyltryptophan
gamma-glutamyltyrosine
gamma-glutamylvaline
Scaled intensity
C S L C S L
DII
Post-DII

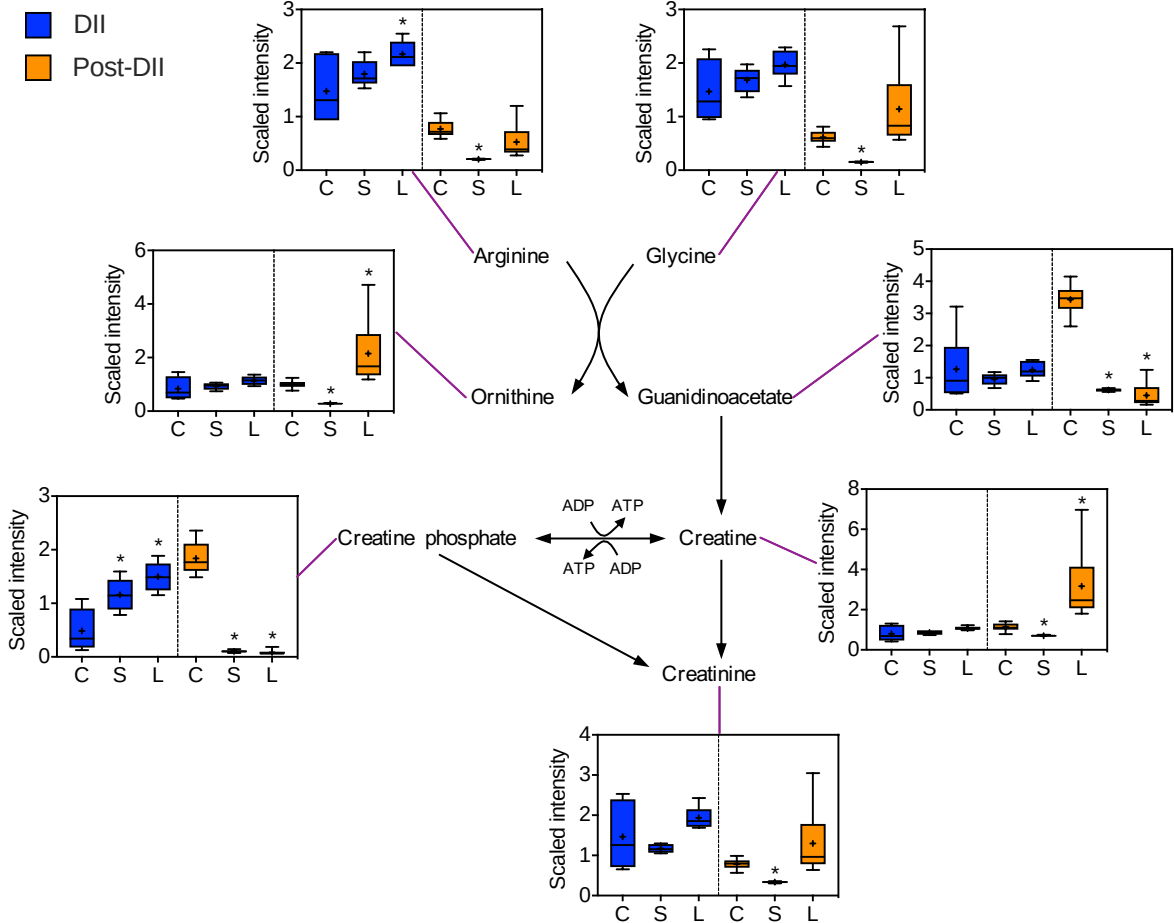
DII
Post-DII
Scaled intensity
C S L C S L
Arginine
Glycine
Ornithine
Guanidinoacetate
Creatine phosphate
ADP ATP
ATP ADP
Creatine
Creatinine

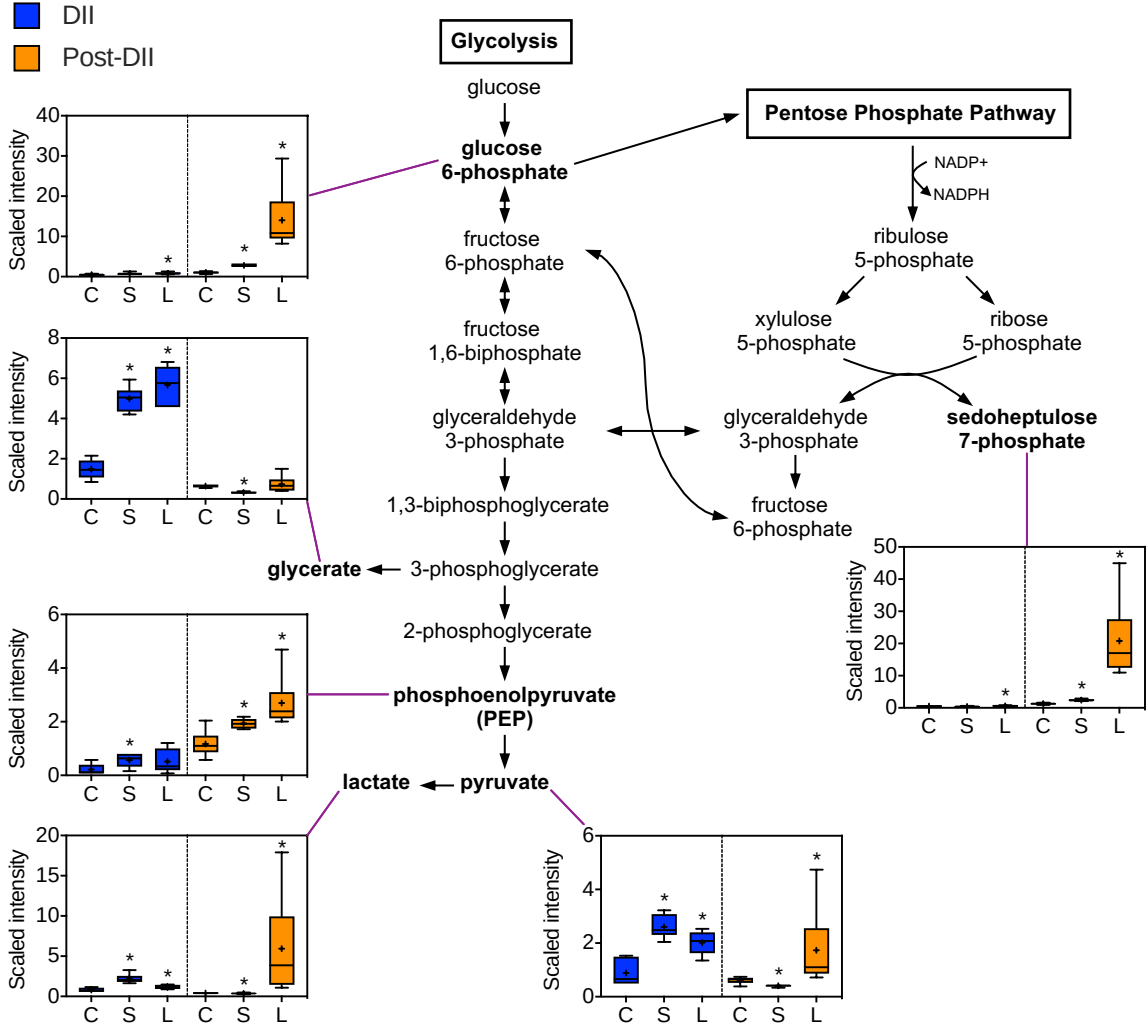
DII
Post-DII
Glycolysis
glucose
glucose 6-phosphate
fructose 6-phosphate
fructose 1,6-biphosphate
glyceraldehyde 3-phosphate
1,3-biphosphoglycerate
glycerate
3-phosphoglycerate
2-phosphoglycerate
phosphoenolpyruvate (PEP)
lactate
pyruvate
Pentose Phosphate Pathway
NADP+
NADPH
ribulose 5-phosphate
xylulose 5-phosphate
ribose 5-phosphate
glyceraldehyde 3-phosphate
sedoheptulose 7-phosphate
fructose 6-phosphate
Scaled intensity
C S L C S L

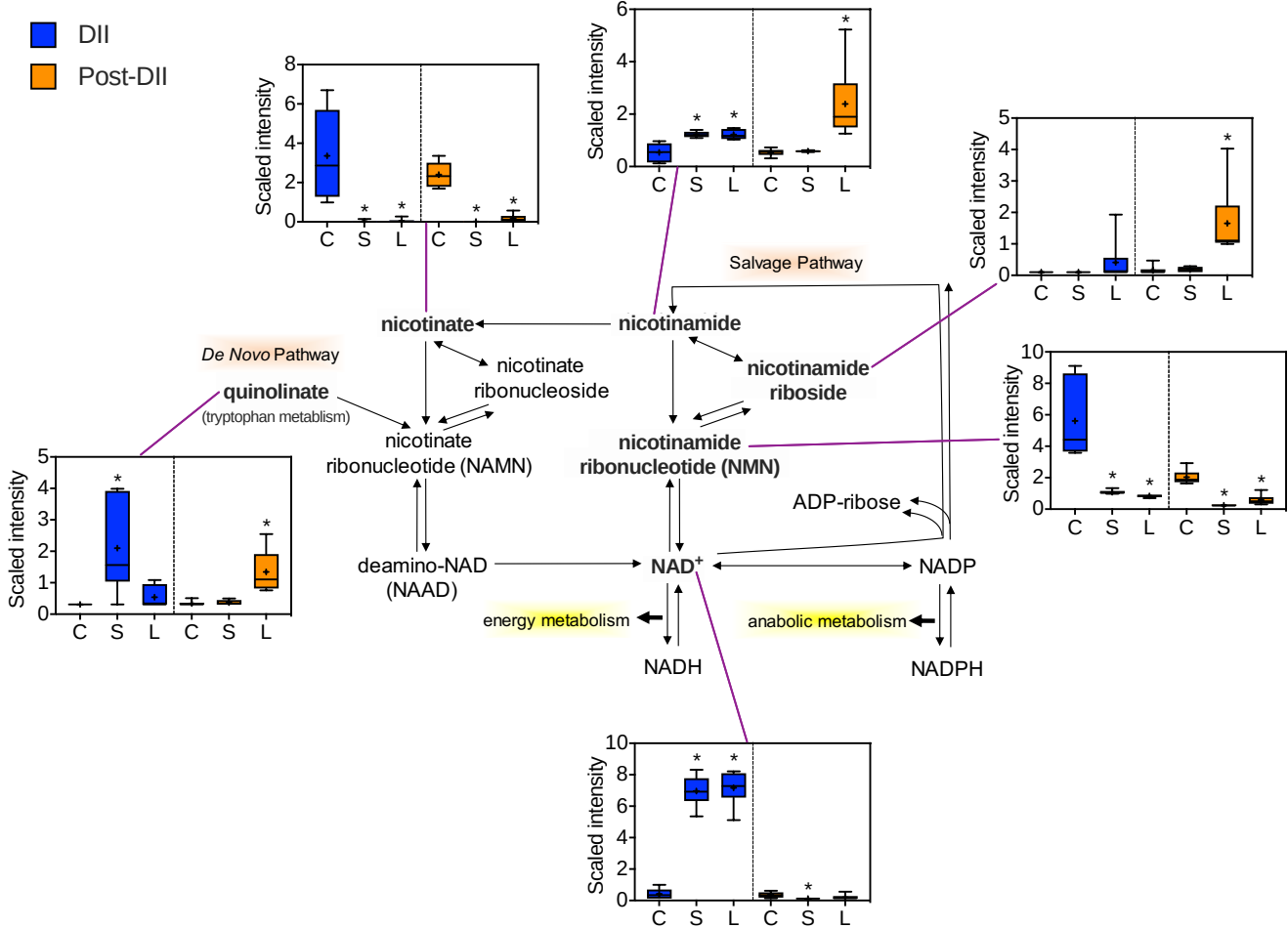
DII
Post-DII
Scaled intensity
C S L C S L
Salvage Pathway
nicotinate
nicotinamide
De Novo Pathway
quinolinate
(tryptophan metablism)
nicotinate ribonucleoside
nicotinamide riboside
nicotinate ribonucleotide (NAMN)
nicotinamide ribonucleotide (NMN)
ADP-ribose
deamino-NAD (NAAD)
NAD+
NADP
energy metabolism
anabolic metabolism
NADH
NADPH

Table 1. Total number of significant metabolites (among 673 total metabolites identified) that were significantly affected by short and long-term aerial dehydration stress in DII and post-DII embryos initially exposed at WS 36.

Stage	Comparison	Non-normalized		Protein-normalized		DNA-normalized	
		Total metabolites $P < 0.05$	Metabolites (up | down)	Total metabolites $P < 0.05$	Metabolites (up | down)	Total metabolites $P < 0.05$	Metabolites (up | down)
DII	7 d / 0 d (short-term)	243	156 | 87	238	85 | 153	204	174 | 30
	28 d / 0 d (long-term)	346	298 | 48	200	77 | 123	267	233 | 34
Post-DII	7 d / 0 d (short-term)	466	383 | 83	438	269 | 169	553	74 | 479
	18 d / 0 d (long-term)	558	430 | 128	544	354 | 190	390	212 | 178

Table 2. Metabolic pathways that were significantly enriched by short and long-term aerial dehydration stress in DII and post-DII embryos normalized to DNA concentration.

Treatment (# significant metabolites)	Subpathway	Enrichment Value	P-value	k	m
DII short-term (n = 204)	Fatty Acid, Dihydroxy	3.3	0.03	3	3
	Fatty Acid, Dicarboxylate	2.6	6.34E-04	10	13
	Fatty Acid, Monohydroxy	2.4	0.03	5	7
	Nicotinate and Nicotinamide Metabolism	2.4	0.03	5	7
	Tyrosine Metabolism	2.4	0.01	7	10
	Methionine, Cysteine, SAM and Taurine Metabolism	2.0	4.17E-03	13	22
	Leucine, Isoleucine and Valine Metabolism	1.9	0.02	11	20
DII long-term (n = 267)	Fatty Acid Metabolism (Acyl Carnitine, Long Chain Saturated)	1.9	0.05	6	8
	Tyrosine Metabolism	1.8	0.05	7	10
	Monoacylglycerol	1.7	0.03	11	17
	Methionine, Cysteine, SAM and Taurine Metabolism	1.6	0.02	14	22
Post-DII short-term (n = 553)	Phosphatidylcholine (PC)	1.2	0.02	19	19
	Urea cycle; Arginine and Proline Metabolism	1.2	0.02	19	19
	Gamma-glutamyl Amino Acid	1.2	0.03	17	17
	Monoacylglycerol	1.2	0.03	17	17
	Diacylglycerol	1.2	7.71E-03	34	35
Post-DII long-term (n = 390)	Aminosugar Metabolism	1.7	0.01	8	8
	Purine Metabolism, Adenine containing	1.6	0.03	9	10
	Gamma-glutamyl Amino Acid	1.5	7.36E-03	15	17
	Monoacylglycerol	1.5	7.36E-03	15	17
	Phosphatidylcholine (PC)	1.5	0.01	16	19

Enrichment value was computed as follows: (k/m)/((n-k)/(N-m)), where: k, total number of significant metabolites in pathway; m, total number of detected metabolites in pathway; n, total number of significant metabolites; N, total number of detected metabolites (673). A pathway enrichment value greater than one indicates that the pathway contained more significantly changed metabolites relative to the study overall. Fisher's exact test was used to determine if pathway enrichment was significant ($P < 0.05$*).*